Journal of
Synchrotron Radiation

ISSN 0909-0495

Received 3 March 2009
Accepted 16 September 2009

Achievements in high-pressure science at the high-brilliance energy-dispersive X-ray absorption spectrometer of ESRF, ID24

Giuliana Aquilanti,*‡ Olivier Mathon and Sakura Pascarelli

ESRF, 6 rue Jules Horowitz, 38043 Grenoble, France. E-mail: giuliana.aquilanti@elettra.trieste.it

Although the idea of an X-ray absorption spectrometer in dispersive geometry was initially conceived for the study of transient phenomena, the instrument at the European Synchrotron Radiation facility has been increasingly exploited for studies at extreme conditions of pressure using diamond anvil cells. The main results of investigations at high pressure obtained at beamline ID24 are reviewed. These concern not only fundamental topics, such as the local and the electronic structure as well as the magnetic properties of matter, but also geological relevant questions such as the behaviour of Fe in the main components of the Earth's interior.

Keywords: energy-dispersive XAS; high pressure; diamond anvil cell.

1. Introduction

The thermodynamic variable pressure is being increasingly employed to study the behaviour of matter when atoms are brought closer to each other. This allows experimental verification of the different models used to describe the structural and the electronic properties of matter. For magnetic materials, the volume occupied by a magnetic atom drives its microscopic properties through its hybridization with its neighbours. Applying high pressure (HP) is the best way to modify the volume and therefore to tune the hybridization. If diffraction methods are still the predominant HP techniques for structural studies involving synchrotron radiation, X-ray absorption spectroscopy (XAS) offers a complementary description of matter under pressure: on one side it gives a local picture since it probes, with chemical selectivity, the local environment around the photoabsorber atom; on the other side it is sensitive to pressure-induced electronic transitions since it probes the electronic density of states above the Fermi level. For magnetic systems presenting a net magnetization, polarized XAS contains additional magnetic information. Indeed, X-ray magnetic circular dichroism (XMCD) is an orbital moment sensitive probe, and owing to the spin–orbit interaction it is also sensitive to spin. HP XMCD is therefore an excellent tool to probe the variation of the magnetic properties with increasing hybridization between a specific atom and its neighbours.

X-ray absorption spectroscopic techniques owe their popularity to the increased worldwide availability of synchrotron sources. Besides the conventional scanning X-ray absorption technique, the interest for energy-dispersive X-ray absorption spectroscopy (EDXAS) has been growing steadily from the early 1980s. Historically, energy-dispersive spectrometers were developed for time-resolved studies since the possibility of collecting the data in parallel over the full energy range of the XAS spectrum makes the dispersive scheme particularly suited to monitoring dynamical processes (*e.g.* Matsushita & Phizackerley, 1981). Nonetheless, compared with the conventional point-by-point approach, recording X-ray absorption spectra in a dispersive mode has several features that make this method advantageous for HP studies using diamond anvil cells (DACs). In fact, the absence of mechanical movements during the acquisition of the spectra and the focusing properties of the polychromator yield the spot stability and dimensions, respectively, required for extremely small samples contained in DACs. In addition, the high-brilliance X-ray beams of third-generation synchrotron sources allow the strong absorption of diamond anvils at low energies (< 9 keV) to be overcome enabling the investigation of all the K and L absorption edges in 3d metals and 4f rare earths. Beamline ID24 is the ESRF's energy-dispersive EXAFS beamline (Hagelstein *et al.*, 1993, 1997; Pascarelli *et al.*, 1999*a*, 2004, 2006). It is the only beamline of its kind to be installed on an undulator source, exploiting the high brilliance and flux of a third-generation synchrotron source. A sketch of the energy-dispersive set-up is shown in Fig. 1 and the optical scheme of beamline ID24 is reported by Pascarelli *et al.* (2006). The tapered undulator source and the chosen optical scheme of ID24 allow us to cover an operation range between 5 and 25 keV. The energy range ΔE diffracted by the polychromator is directly proportional to the footprint of the beam on the polychromator and to the cotangent of the Bragg angle ($\Delta E = \Delta\theta \cot\theta$). Typical values for $\Delta E/E$ range between 5% and 15% at low and high energies, respectively. Nonetheless,

‡ Present address: Sincrotrone Trieste, Elettra Light Source, SS 14, km 163.5, 34149 Basovizza, Trieste, Italy.

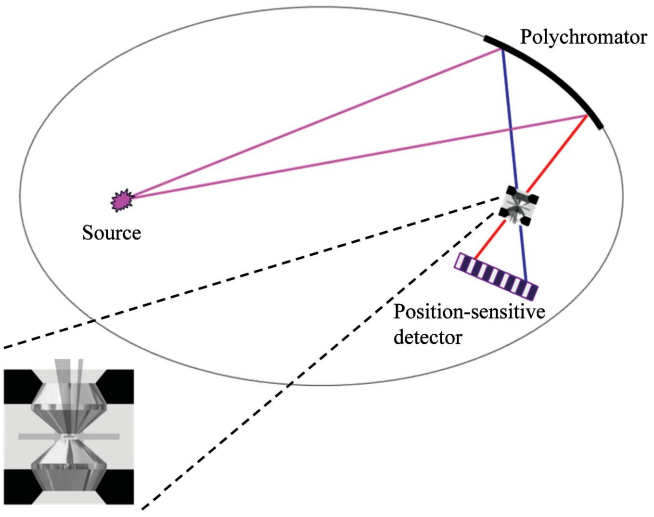

Figure 1
A quasi-parallel and polychromatic beam, supplied by a synchrotron radiation source, is energy dispersed and focused by an elliptical curved crystal. Since the incident X-rays strike the crystal at slightly different angles along its length, the bent crystal acts as a polychromator diffracting at different energies at each point. The energy-dispersed beam converges to a point where the sample (for example in a DAC) is placed. The beam, transmitted through the sample, then diverges towards a position-sensitive detector. The source and the image are at the two foci of an ellipse. The position of the beam, on the detector, can be directly correlated to energy. By measuring the spatial X-ray intensity in the presence (I_1) and absence (I_0) of the sample, an X-ray absorption spectrum can be consequently obtained by taking the logarithm of the ratio of the I_0 and I_1 data. Inset: scheme of a DAC.

at energies above ∼10 keV the limitation of the spectra *k*-range is due to the occurrence of the Bragg diffraction peaks that remain the main limit to the exploitation of the high-pressure XAS data recorded using DACs (Aquilanti *et al.*, 2009). Fig. 2 shows how the *k*-range of the high-pressure XAS using DACs varies with working energy. The time resolution naturally provided by the dispersive optics offers the advantage to obtain, in a reasonable time, a relatively large diffraction reflection-free energy bandpass by following online the transmitted beam on the two-dimensional detector as a function of diamond orientation.

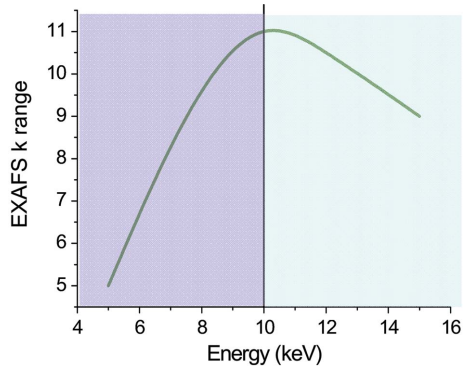

Figure 2
k-range of EXAFS data recorded at ID24 using a DAC as a function of the working energy. In the energy range highlighted in purple (darker shading) the limitation is due to the large incident angle θ on the polychromator, while in the energy range highlighted in pale blue (lighter shading) it is due to the Bragg reflections from the diamonds.

Since the start of operation a constant optimization and refurbishing program has been carried out yielding a steady growth of the in-house and users research activity at HP, and instrumentation developments were fundamental to reach the present performance of the ID24 instrument (Pellicer-Porres *et al.*, 1998; Pascarelli *et al.*, 2004). Results from HP science cover very diverse fields of research. The bulk of HP studies concerns fundamental physics such as the evolution with increasing density of the local structural and electronic properties of oxides, semiconductors and metals. The intrinsic fast acquisition speed and spot stability of the EDXAS spectrometer together with efforts to improve the optical components of beamline ID24, leading to a focal spot size of 5 µm × 5 µm FWHM, opened the way to new fields of research. The study of heterogeneous and geological-relevant materials at HP was undertaken with a 5 µm spatial resolution obtaining maps where each pixel contains full XAS information. Moreover, the above-mentioned characteristics of ID24 together with the optimization of the data acquisition strategy allowed the detection of very small signals such as X-ray magnetic circular or linear dichroism (XMCD or XMLD) at HP, where the effect of pressure on magnetic ordering or on magnetoelastic coupling could be investigated.

In this paper we report the most significant results of HP studies undertaken in the last ten years at beamline ID24, ESRF. The paper is organized as follows. In §2 we will overview the results of structural XAFS studies at HP highlighting the complementarity of XAFS with respect to X-ray diffraction (XRD) techniques. In §3 we will illustrate two examples in which XAS contributes to the knowledge of the evolution of the electronic properties of matter as a function of pressure. In §4 we discuss the evolution of the interatomic distances in a molecular system such as bromine. In §5 we will review the HP studies on magnetic materials. We will show how the differential XAFS techniques (*i.e.* XMLD and XMCD) at HP are excellent tools to probe the variation of the magnetic properties with increasing pressure and how these are related to structural modifications. In §6 we will illustrate the emerging applications of beamline ID24 and show the first results concerning Fe partitioning on a complex geophysical-relevant chemical system. In §7 we briefly illustrate some of the future opportunities of the EDXAS spectrometer of the ESRF for studies at extreme conditions.

2. Structure

2.1. Semiconductors

A large part of the studies undertaken at ID24 concerns the evolution of the local structure of semiconductors. A group of these studies are related to the layered structured semiconductors such as GaTe, InSe and GaSe (Pellicer-Porres *et al.*, 1999, 2000, 2002; Segura *et al.*, 2003). These materials have been proposed in the development of solar cells, non-linear optics or as candidates for solid-state batteries. They also represent an exciting and challenging training ground for the development of models capable of simultaneously describing

electronic interactions of very different nature. Having highly anisotropic physical properties under HP, the strength of intralayer and interlayer interactions evolve in a drastically different manner. The layered character of such systems, on one side, makes it very difficult to obtain a pure single-crystalline sample, and on the other side introduces preferential orientation in powder samples. As a consequence, it is critical to retrieve the pressure evolution of the atomic positions in the unit cell. Taking advantage of the linearly polarized character of synchrotron radiation, it has been shown that not all intralayer distances scale with the cell parameter *a* as it was previously believed. This result changed the previously accepted view, invalidating the intralayer and interlayer deformation potential (Kuroda *et al.*, 1986; Gauthier *et al.*, 1989) used to explain the evolution of the band structure under pressure. In addition, under plausible hypothesis according to which the cation–cation bond compressibility is close to the cation–anion one, it was possible to give the evolution of the whole structure under pressure.

Less exotic with respect to the layered structured, but nonetheless very popular in the HP research, are the octet compounds $A^nB^{(8-n)}$. This class of materials has attracted much attention in the past few years both for experimentalists and theoreticians (Nelmes & McMahon, 1998; Mujica *et al.*, 2003). A re-evaluation of the structural sequence was proposed during the 1990s with the identification of *Cmcm* as a common structure at high pressure (Nelmes *et al.*, 1997). In many cases, however, the full description of the high-pressure phases remained uncertain, owing to the difficulty of addressing the problem of chemical ordering using diffraction techniques alone. This issue derived from the difficulties in obtaining correct hydrostatic conditions within the DAC, leading to progressive widening of the diffraction peaks with pressure and therefore to a lower sensitivity of the technique to site occupancy. In the framework of a structural high-pressure study of III–V semiconductors we have performed XAS measurements on GaP and InAs up to 39 and 80 GPa, respectively (Pascarelli *et al.*, 2002, 2003; Aquilanti & Pascarelli, 2005; Aquilanti, Libotte *et al.*, 2007). For GaP, although XRD shows the presence of chemical disorder, our X-ray absorption near-edge spectra (XANES) and their comparison with state-of-the-art full multiple scattering calculations confirm unequivocally the occurrence of a *Cmcm* symmetry with a high degree of local chemical ordering (Fig. 3). For InAs we were able to perform a full EXAFS analysis and determine the evolution of the local structure up to 80 GPa. While up to 31 GPa the local environment around As is given by six In atoms in full agreement with XRD results, for the data above 31 GPa models based on a local environment of six In atoms only must be excluded, and our results show that a non-negligible additional contribution of As atoms, the coordination number of which increases with pressure, is observed. Fig. 4 shows a comparison between the experimental EXAFS function for the data at 52 GPa and the theoretical best-fit results and the single As–In and As–As contributions. The residual function exceeding the noise level only at low *k* is due to higher shells and to multiple-scattering

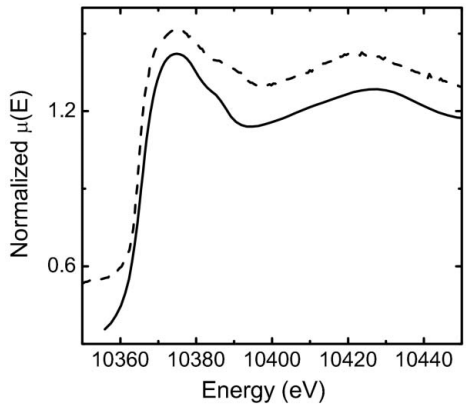

Figure 3
Simulated spectrum of GaP in chemically ordered *Cmcm* structure (full line) and the experimental XANES spectrum at 39 GPa (dashed line) (Aquilanti, Libotte *et al.*, 2007).

contributions. The good agreement at high *k* indicates that the model describing the near neighbour environment given by six In and four As atoms is correct. The local environment of As above 31 GPa is compatible with a *Pmma* structure as determined by XRD. However, the measured coordination of As (As–As interactions) using a local and chemically sensitive method, such as EXAFS, is higher than that present in the *Pmma* phase derived by XRD. Therefore, InAs at high pressure presents a local environment around As that is chemically disordered. This behaviour must be considered in relation to that obtained for GaP whose ionicity is lower than that of InAs. The two results suggest that ionicity dictates the behaviour of the short-range interaction only up to a certain pressure, above which the *pV* term in Gibbs free energy,

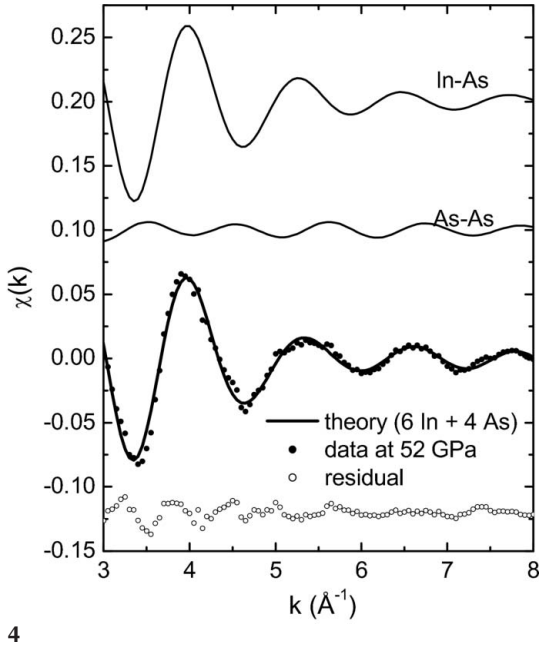

Figure 4
Solid curves: from top to bottom, best-fit calculations corresponding to the In–As, As–As, total signal and residual. The total signal is directly compared with the experimental EXAFS function (dots) (Aquilanti & Pascarelli, 2005).

$G = E + pV - TS$, determines the nature of the chemical bonds and the possible formation of new homopolar bonding that is forbidden at lower pressures owing to hindrance by the ionicity of the bonds.

2.2. Scheelite-structured compounds

In some cases XAS played the role of referee in long-standing debates. The scheelite ABX_4 compounds, of which the tungstates AWO_4 are a sub-branch, constitute a large family of materials that are important from a technological point of view. Upon compression, most of these compounds have been reported to undergo structural transitions to monoclinic structures. A comprehensive review on pressure effects on structural and electronic properties of ABX_4 can be found by Errandonea & Manjón (2008). However, several of these low-symmetry structures have proved difficult to characterize in HP XRD experiments and it has been suggested that their formation could be sensitive to the stress conditions in the pressure chambers. In such cases, XAS can play an important complementary role in identifying the structures of the new phases as it is less sensitive to non-hydrostaticity and uniaxial strain, since it measures average bond distances directly. Recently, new diffraction data have been recorded of $CaWO_4$, $SrWO_4$, $BaWO_4$ and $PbWO_4$ (Errandonea *et al.*, 2005, 2006). A scheelite-to-fergusonite phase transition has been observed and state-of-the-art XANES calculations compared with experimental XANES data confirmed this scenario, not only making the XRD result more reliable but also closing the debate on the high-pressure stability in these compounds.

3. Electronic structure: pressure-induced isostructural transitions

3.1. Intercalated clathrates

A material that has been investigated at HP at ID24 is the intercalated clathrate Ba_8Si_{46}. Properties of type-I silicon clathrates at high pressure are motivated by both fundamental and applied reasons (San Miguel, 2006). These zeolite-type materials show a set of intriguing phase transitions which could be made part of a general phenomena in nano-intercalated systems. It has been shown that Ba_8Si_{46} undergoes a pressure-induced isostructural transition with a homotectic volume contraction. In all of the cases where isostructural homothetic transitions have been reported, pressure-induced electron transfer was invoked as the driving mechanism of the isostructural transition. In order to verify this hypothesis, XANES at the Ba L_3-edge were measured to a pressure up to 20 GPa (San Miguel *et al.*, 2005). The X-ray absorption white line shows a discontinuity in the evolution of its width at 11–12 GPa that can be linked either to a modification of the electronic structure related to the Ba–Si hybridization or to a more disordered environment around Ba atoms. Such a discontinuity was also associated with modifications of the vibration pattern detected by Raman spectroscopy, and interpreted as a signature of the displacement of Ba atoms from the centre of the Si_{24} cages (Kume *et al.*, 2003).

3.2. Electronic topological transition on metallic zinc

Another example in which an XAS study performed at ID24 contributed to understand fundamental issues of condensed matter physics concerns metallic zinc under HP. Metallic zinc is an intriguing system since, together with its electronic counterpart metallic cadmium, it is unique among divalent hexagonal-close-packed (h.c.p.) structured metals as the *c*/*a* axial ratio exceeds about 14% of the ideal value of h.c.p. structures. This anomaly makes many of its solid-state properties highly anisotropic and at high pressure Zn is believed to undergo a Lifshitz or electronic topological transition (ETT) near 10 GPa. This type of phase transition arises when distortion of the electronic band structure owing to an external agent such as doping, hydrostatic pressure or anisotropic strain modifies the topology of the Fermi surface. For this reason, compressed zinc has been extensively studied both theoretically and experimentally with a disconcerting plethora of different results. In particular, X-ray diffraction of Zn under pressure has shown to be particularly sensitive to hydrostatic conditions (Takemura, 1995, 1997, 1999; Takemura *et al.*, 2002). We have studied compressed metallic zinc using EDXAS at ID24 under different hydrostatic conditions (Aquilanti, Trapananti *et al.*, 2007). The main aim of this study was to give direct evidence of the ETT in solid Zn under pressure by probing the variation of the XANES. In fact, according to the electric dipole selection rules, the XANES spectra directly probe the density of unoccupied states with *p* symmetry. Therefore, the variations as a function of pressure of the near-edge structures of the spectra are a probe of pressure-induced changes in the electronic density of states above the Fermi level and may be direct evidence of the ETT. Fig. 5 shows the near-edge part of the spectra of the experiment undertaken using 4:1 methanol:ethanol and neon as pressure-transmitting media. The gradual evolution with pressure of the XANES features for the two experiments with different hydrostatic conditions not only shows no evidence of

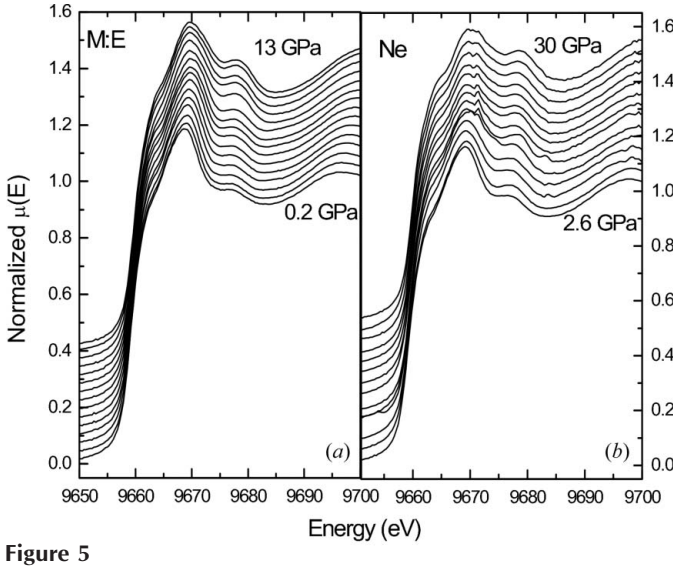

Figure 5
XANES spectra using methanol:ethanol 4:1 (*a*) and Ne (*b*) as pressure-transmitting medium (Aquilanti, Trapananti *et al.*, 2007).

an electronic transition in Zn under pressure but also demonstrates that since XAS measures average bond distances directly it is less sensitive to non-hydrostaticity, allowing a reliable answer to be obtained independently of small variations of hydrostatic conditions which are very often difficult to control in high-pressure studies using DACs.

4. Molecular systems

4.1. The case of bromine

The case of bromine falls again into the field of fundamental research even though the behaviour under compression of heavier halogens such as Br_2 and I_2 (*i.e.* metallization or dissociation) can be taken as a model for other molecular solids such as O_2 and H_2 which are of central interest both from a theoretical point of view and for their implications in astrophysical problems. Bromine has a layered structure and each layer consists of in-plane molecules arranged in a zig-zag configuration. Interactions between the layers are of van der Waals type leading to bonds that are most easily squeezed under pressure. Therefore the distance between the layers decreases rapidly with pressure. On the other hand, the intramolecular distances remain constant or slightly increase owing to a charge transfer effect from within the molecule towards the interplanar region. XRD on bromine shows an intramolecular distance which remains constant within the error bars up to above 80 GPa. The experimentally extracted $\chi(k)$ function is shown in Fig. 6(*a*) for some selected data. At low pressure the main contribution to the signal is given by the scattering of the Br atom inside the molecule, while at higher pressure contributions from the second and higher neighbouring shells become increasingly important. EXAFS, owing to its high resolution at very short distances, showed not only an evolution of the intramolecular distance with compression but also, and more interestingly, evidenced that the distance first elongates to 0.06 Å and then suddenly contracts at 25 GPa as shown in Fig. 6(*b*) (San Miguel *et al.*, 2000, 2007). This behaviour is accompanied by a discontinuity of the FWHM of the pre-edge peak. The combination of these effects highlights a phase transition in solid bromine at 25 GPa not detected by XRD. This phase transition, associated with a sudden change in the molecular character of the structure of Br_2, can be extended to other molecular systems. Yet, the exact nature of the observed phase transition, which appeared to be associated with modifications in the electronic structure, remains to be clarified and more theoretical investigations are called for.

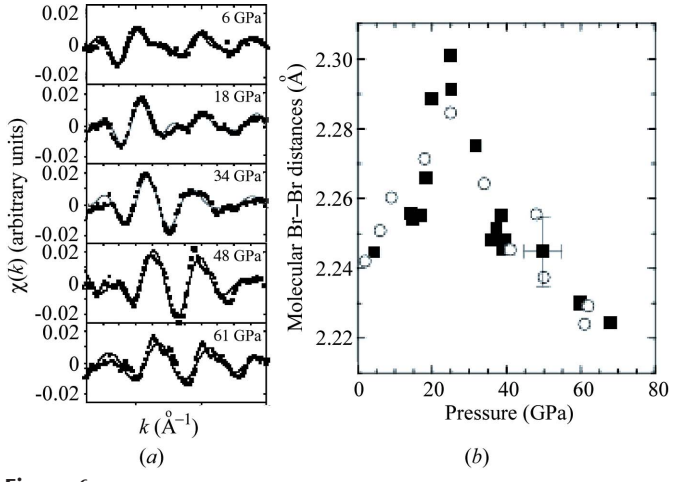

Figure 6
(*a*) EXAFS oscillations at the bromine *K*-edge as a function of pressure (dots) and their fit (lines). (*b*) Intramolecular distance evolution obtained from EXAFS analysis. The different symbols are related to two different runs. Up to 25 GPa the elongation of Br_2 increases and then a phase transition takes place (San Miguel *et al.*, 2007).

5. Magnetism

A number of experiments on ID24 have exploited the linear and circular polarization of synchrotron radiation to probe the effect of pressure on magnetism in 3*d* metals using XMCD and XMLD.

In ferromagnetic Fe, Co, Ni and their alloys, the partial filling of narrow 3*d* bands following Hund's rules, and high electron density near the Fermi level results in a spin-polarized valence band. In these 3*d* metals magnetism plays a fundamental role. For example, it greatly influences the structural properties in stabilizing body-centred-cubic (b.c.c.) Fe and h.c.p. Co instead of h.c.p. Fe and face-centred-cubic (f.c.c.) Co predicted without spin polarization.

The magnetic properties of 3*d* metals and their alloys have also become the subject of intensive theoretical and experimental research because of the technological implications for high-density magneto-optical storage media. An essential parameter to further increase the recording density in hard disk drives is a large uniaxial magnetocrystalline anisotropy (MCA). Recent *ab initio* calculations have shown that when the cubic lattice symmetry of ferromagnetic homogeneously disordered alloys is broken, *i.e.* by imposing a compositional modulation or a tetragonal distortion, MCA is largely enhanced. These results show how even subtle changes in the local chemical environment and in local structure can deeply modify magnetic properties.

Application of pressure is an effective way of studying the complex interplay between magnetic and structural degrees of freedom, because pressure acts directly on interatomic distances. In particular, under pressure the steeper increase in electron kinetic energy *versus* potential energy diminishes the importance of Coulomb correlations. Accordingly, at sufficiently high pressures, Fe, Co and Ni are all presumed non-correlated metals although this has been experimentally verified only in the case of Fe.

Using XMCD, the effect of pressure on Fe and its compounds is seen to induce important magnetic instabilities that lead to structural phase transitions to non-ferromagnetic phases (Mathon *et al.*, 2004) or to partial suppression of magnetic moments (Duman *et al.*, 2005). The rapid or gradual suppression of long-range magnetic order can be explained by pressure-induced broadening of the electronic bands leading to an enhancement of 3*d*–4*p* hybridization, contributing to a

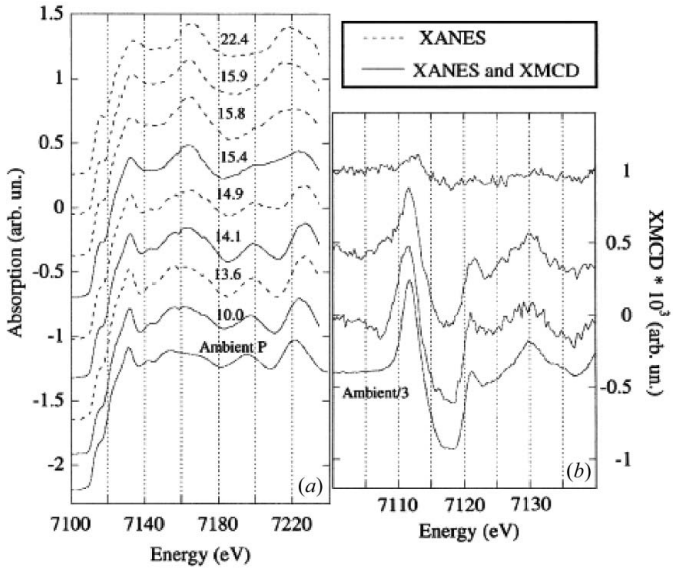

Figure 7
Fe *K*-edge XAS (*a*) and some examples of XMCD (*b*) as a function of pressure between the ambient-pressure b.c.c. phase and the high-pressure h.c.p. phase. Continuous lines correspond to examples of data measured simultaneously. The small glitches in the XAS at 7158 and 7171 eV in the high-pressure data are artifacts owing to small defects of the polychromator crystal (Mathon *et al.*, 2004).

lower density of states at the Fermi level such that the magnetic state stability condition given by the Stoner criterion is no longer met.

The Fe b.c.c. to h.c.p. phase transition has been investigated in detail using simultaneous XMCD and XANES (Mathon *et al.*, 2004): the combination of the two techniques allowed us to obtain simultaneously information on both the structure and the magnetic state of compressed Fe (Fig. 7). The magnetic and structural transitions are both sharp and of first order in agreement with the theoretical prediction. The pressure domain of the transition observed, 2.4 ± 2 GPa, is narrower than that usually cited in the literature (8 GPa). Our data suggested that the magnetic transition slightly precedes the structural one. If this effect were to be confirmed by future measurements, it could mean that the origin of the instability of the b.c.c. phase in Fe with increasing pressure is to be attributed to the effect of pressure on magnetism, and not to phonon instabilities of the b.c.c. phase, as predicted by spin-polarized full-potential total energy calculations.

As an example of a high-moment to low-moment transition induced by pressure, we can cite the case of the ferromagnetic interstitial iron compound Fe_3C (cementite). Cementite is expected to have Invar properties, whereby a high-moment to low-moment transition should occur when the atomic volume is reduced below a critical value. We examined the pressure dependence of the Fe *K*-edge XMCD in Fe_3C at ambient temperature and pressures up to 20 GPa (Fig. 8*a*) (Duman *et al.*, 2005) and found evidence for a high-moment to low-moment transition around 10 GPa (Fig. 8*b*). This magnetovolume instability is expected to be the source of the Invar-typical features observed in the temperature dependence of the thermodynamical parameters for this material. However, how the properties of the instability are related to the local characteristics of the two individual Fe sites (FeI and FeII) remain presently unanswered. To gain more information, it is necessary to provide more elaborate modelling for *K*-edge XMCD spectroscopy of Fe and Fe_3C. Also, to decide whether the Invar effect in Fe_3C can be explained within the framework of a two-state high-moment low-moment model, as for $Fe_{0.64}Ni_{0.36}$, or within a framework that relates the cause to a presence of disordered magnetic moments requires further investigation.

Pressure has also been used as an important degree of freedom in the investigation of magnetoelastic coupling in 3*d* metal alloys (Pascarelli *et al.*, 2007). Using XMLD, we have studied the effect of pressure on femtometre-scale bond strain owing to anisotropic magnetostriction in a thin FeCo film. These kinds of experiments have become possible owing to recent advances in beam stability and detection on ID24, allowing a sensitivity in atomic displacements of the order of the femtometre to be reached (Pettifer *et al.*, 2005). In FeCo, local magnetostrictive strain is found to increase upon compression in agreement with spin-polarized *ab initio* electronic structure calculations, but contrary to the expected effect of compression on bond stiffness. Evidently the pressure-induced broadening of the *d* bands contributes to an enhancement of the distortion-induced band shifting and

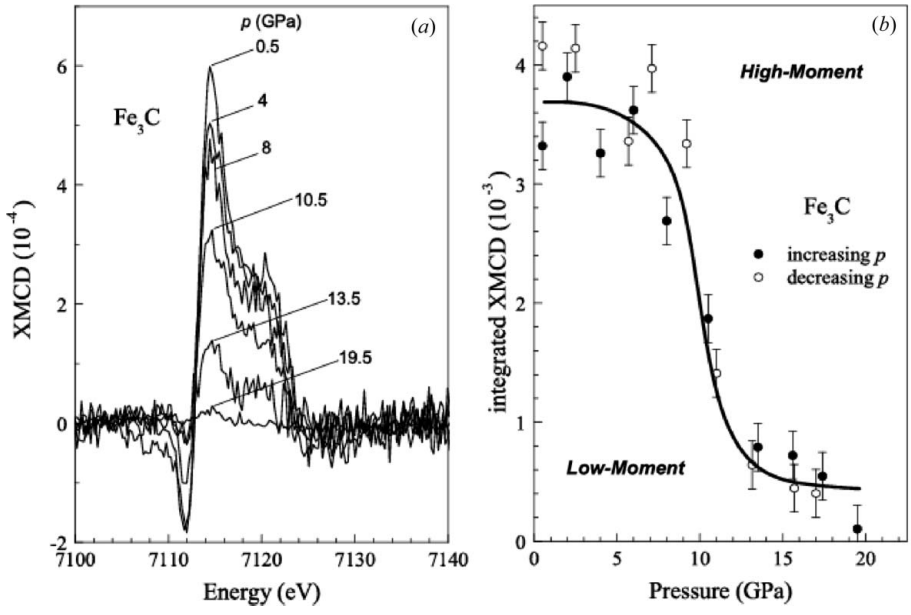

Figure 8
(*a*) XMCD of Fe_3C around the Fe *K*-edge at selected pressures. (*b*) Integrated XMCD of Fe_3C. The high-moment to low-moment transition takes place at about 10 GPa (Duman *et al.*, 2005).

broadening, which is responsible for the positive magnetostriction constant in FeCo, and leads to a higher sensitivity of MCA to strain. If a three-dimensional compression of bulk FeCo obtained through the application of hydrostatic pressure enhances magnetostriction, then one could expect similar effects in thin epitaxically grown FeCo films where lattice mismatch plays a similar role as the application of pressure along two dimensions.

6. Emerging applications

The evolution of the optical elements on ID24 allowed a spot size of 5 μm × 5 μm FWHM to be achieved (Pascarelli *et al.*, 2006). This spot size, coupled with fast data acquisition, leads to the possibility of recording μ-XANES maps with a spatial resolution of a few micrometres, where each pixel contains full XANES information. Initially this method was predominantly associated with fluorescence detection (Pascarelli *et al.*, 1999*b*) to investigate the content, redox and speciation of iron on natural rock thin sections (Muñoz *et al.*, 2006; Vidal *et al.*, 2006), or for the understanding of the main factors responsible for the crystallization of minerals (Andreáni *et al.*, 2008). This method has then been extended to investigations in the transmission mode within a DAC (Aquilanti *et al.*, 2009) to probe the potential of μ-XAS mapping for *in situ* studies at extreme conditions of pressure and temperature. The case study was the investigation of the behaviour of iron during the decomposition of (Mg,Fe)-ringwoodite into silicate perovskite and ferropericlase, which occurs at the upper/lower mantle boundary. Indeed, because of its abundance and its different oxidation state, iron is one of the major elements governing the past and present of our planet (Wood *et al.*, 2006), and knowledge of its speciation in the different crystalline phases of the mantle is fundamental. The chemical reaction of geophysical interest that we have explored was $(Fe_{0.12},Mg_{0.88})_2SiO_4 \rightarrow (Fe_x,Mg_{1-x})SiO_3 + (Fe_y,Mg_{1-y})O$ with $x = 0.24 - y$, occurring at ∼23 GPa and 1900 K. The occurrence of this reaction would explain the abrupt changes of the properties of the Earth's interior at 660 km below the surface, such as the increase of both density and transmission speed of seismic waves owing to earthquakes. In this experiment the DAC was scanned horizontally and vertically in the focal plane of the X-rays with steps of 5 μm. Fe *K*-edge XANES were recorded over a 40 × 40 step grid in order to cover an area of 200 μm × 200 μm. Each map contained 1600 XANES spectra (one spectrum per pixel) and was recorded in ∼100 min. μ-XANES maps were recorded at 26 GPa before and after laser heating, and at 37 GPa after laser heating. The sample was laser heated at a spot in the centre of the sample at 1900 K. The data were automatically processed to retrieve two-dimensional maps using the *XASMAP* software (Muñoz *et al.*, 2006). The μ-XANES maps were successively analyzed using an analytical procedure illustrated by Muñoz *et al.* (2008). This procedure includes standard-deviation principal component analysis and multicomponent linear-combination fits. We have shown how this method can assess, with micrometric spatial resolution, the chemistry of individual high-pressure phases in a complex chemical system such as that of the Earth, with the possibility of providing information about the oxidation state and speciation of the probed element at high temperature and pressure conditions.

7. Future opportunities

As future opportunities for science at extreme conditions, EDXAS can give a contribution to the study of molten elements at HP using the laser-heated DAC. Thermodynamic conditions of melting under high pressure, as well as the local structure in the melt, are of great interest in different fields ranging from fundamental physics to planetary interior studies. The dimensions of samples best suited to be molten has to be commensurate with the size of the laser beam. In addition, data need to be recorded using very short acquisition times in order to probe the sample in a pure liquid phase and to deal with sample and/or temperature fluctuations (Dewaele *et al.*, 2007). These two requirements make EDXAS particularly advantageous for studying melts in the laser-heated DAC and complementary to the laser speckle method and XRD methods.

Again, profiting of the time resolution naturally offered by the EDXAS spectrometer coupled to a high-brilliance source, it will be possible to follow *in situ* the kinetics of chemical reactions or diffusion processes inside a DAC.

Finally, ID24 offers today a unique opportunity to perform time-resolved XAS measurements aimed at probing fundamental fast processes in chemistry, biochemistry and condensed matter. Experiments aimed at studying the dynamics of phase transitions at high pressures, temperatures or magnetic fields together with the implementation of laser shock investigations are a natural extension of the activities on this facility. The observation of absorption-edge shifts and changes in the XANES during shock can provide valuable insight into the electronic structure modifications induced by the shock wave.

References

Andreáni, M., Grauby, O., Baronnet, A. & Muñoz, M. (2008). *Eur. J. Mineral.* **20**, 159–171.

Aquilanti, G., Libotte, H., Crichton, W. A., Pascarelli, S., Trapananti, A. & Itié, J.-P. (2007). *Phys. Rev. B*, **76**, 064103.

Aquilanti, G. & Pascarelli, S. (2005). *J. Phys. Condens. Matter*, **17**, 1811–1824.

Aquilanti, G., Pascarelli, S., Mathon, O., Muñoz, M., Narygina, O. & Dubrovinsky, L. (2009). *J. Synchrotron Rad.* **16**, 376–379.

Aquilanti, G., Trapananti, A., Minicucci, M., Liscio, F., Twaróg, A., Principi, E. & Pascarelli, S. (2007). *Phys. Rev. B*, **76**, 144102.

Dewaele, A., Mezouar, M., Guignot, N. & Loubeyre, P. (2007). *Phys. Rev. B*, **76**, 144106.

Duman, E., Acet, M., Wassermann, E. F., Itié, J. P., Baudelet, F., Mathon, O. & Pascarelli, S. (2005). *Phys. Rev. Lett.* **94**, 075502.

Errandonea, D. & Manjón, F. J. (2008). *Prog. Mater. Sci.* **53**, 711–773.

Errandonea, D., Pellicer-Porres, J., Manjón, F. J., Segura, A., Ferrer-Roca, Ch., Kumar, R. S., Tschauner, O., López-Solano, J., Rodríguez-Hernández, P., Radescu, S., Mujica, A., Muñoz, A. & Aquilanti, G. (2006). *Phys. Rev. B*, **73**, 224103.

Errandonea, D., Pellicer-Porres, J., Manjón, F. J., Segura, A., Ferrer-Roca, Ch., Kumar, R. S., Tschauner, O., Rodríguez-Hernández, P.,

López-Solano, J., Radescu, S., Mujica, A., Muñoz, A. & Aquilanti, G. (2005). *Phys. Rev. B*, **72**, 174106.
Gauthier, M., Polian, A., Besson, J. M. & Chevy, A. (1989). *Phys. Rev. B*, **40**, 3837–3854.
Hagelstein, M., Fontaine, A. & Goulon, J. (1993). *Jpn. J. Appl. Phys.* **32**, 240–242.
Hagelstein, M., San Miguel, A., Fontaine, A. & Goulon, J. (1997). *J. Phys. IV*, **7**(C2), 303–308.
Kume, T., Fukuoka, H., Koda, T., Sasaki, S., Shimizu, H. & Yamanaka, S. (2003). *Phys. Rev. Lett.* **90**, 155503.
Kuroda, N., Ueno, O. & Nishina, Y. (1986). *J. Phys. Soc. Jpn*, **55**, 581–589.
Mathon, O., Baudelet, F., Itié, J.-P., Polian, A., D'Astuto, M., Chervin, J. C. & Pascarelli, S. (2004). *Phys. Rev. Lett.* **93**, 255503.
Matsushita, T. & Phizackerley, R. P. (1981). *Jpn. J. Appl. Phys.* **20**, 2223–2228.
Mujica, A., Rubio, A., Muñoz, A. & Needs, R. J. (2003). *Rev. Mod. Phys.* **75**, 863–912.
Muñoz, M., De Andrade, V., Vidal, O., Lewin, E., Pascarelli, S. & Susini, J. (2006). *Geochem. Geophys. Geosyst.* **7**, Q11020.
Muñoz, M., Pascarelli, S., Aquilanti, G., Narygina, O., Kurnosov, A. & Dubrovinsky, L. (2008). *High Press. Res.* **28**, 665–673.
Nelmes, R. J. & McMahon, M. I. (1998). *Semicond. Semimet.* **54**, 145–246.
Nelmes, R. J., McMahon, M. I. & Belmonte, S. A. (1997). *Phys. Rev. Lett.* **79**, 3668–3671.
Pascarelli, S., Aquilanti, G., Crichton, W., Le Bihan, T., De Panfilis, S., Fabiani, E., Mezouar, M., Itié, J.-P. & Polian, A. (2002). *High Press. Res.* **22**, 331–335.
Pascarelli, S., Aquilanti, G., Crichton, W. A., Le Bihan, T., Mezouar, M., De Panfilis, S., Itié, J.-P. & Polian, A. (2003). *Europhys. Lett.* **61**, 554–560.
Pascarelli, S., Mathon, O. & Aquilanti, G. (2004). *J. Alloys Compd.* **362**, 33–40.
Pascarelli, S., Mathon, O., Muñoz, M., Mairs, T. & Susini, J. (2006). *J. Synchrotron Rad.* **13**, 351–358.
Pascarelli, S., Neisius, T. & De Panfilis, S. (1999*b*). *J. Synchrotron Rad.* **6**, 1044–1050.
Pascarelli, S., Neisius, T., De Panfilis, S., Bonfim, M., Pizzini, S., Mackay, K., David, S., Fontaine, A., San Miguel, A., Itié, J. P., Gauthier, M. & Polian, A. (1999a). *J. Synchrotron Rad.* **6**, 146–148.
Pascarelli, S., Ruffoni, M. P., Trapananti, A., Mathon, O., Aquilanti, G., Ostanin, S., Staunton, J. B. & Pettifer, R. F. (2007). *Phys. Rev. Lett.* **99**, 237204.
Pellicer-Porres, J., San Miguel, A. & Fontaine, A. (1998). *J. Synchrotron Rad.* **5**, 1250–1257.
Pellicer-Porres, J., Segura, A., Ferrer, Ch., Muñoz, V., San Miguel, A., Polian, A., Itié, J.-P., Gauthier, M. & Pascarelli, S. (2002). *Phys. Rev. B*, **65**, 174103.
Pellicer-Porres, J., Segura, A., Muñoz, V. & San Miguel, A. (1999). *Phys. Rev. B*, **60**, 3757–3763.
Pellicer-Porres, J., Segura, A., Muñoz, V. & San Miguel, A. (2000). *Phys. Rev. B*, **61**, 125–131.
Pettifer, R. F., Mathon, O., Pascarelli, S., Cooke, M. & Gibbs, M. (2005). *Nature (London)*, **435**, 78–81.
San Miguel, A. (2006). *Chem. Soc. Rev.* **35**, 876–889.
San Miguel, A., Libotte, H., Gaspard, J.-P., Gauthier, M., Polian, A. & Itié, J.-P. (2000). *Eur. Phys. J. B*, **17**, 227.
San Miguel, A., Libotte, H., Gauthier, M., Aquilanti, G., Pascarelli, S. & Gaspard, J.-P. (2007). *Phys. Rev. Lett.* **99**, 015501.
San Miguel, A., Merlen, A., Toulemonde, P., Kume, T., Le Floch, S., Aouizerat, A., Pascarelli, S., Aquilanti, G., Mathon, O., Le Bihan, T., Itié, J.-P. & Yamanaka, S. (2005). *Europhys. Lett.* **69**, 556–562.
Segura, A., Manjón, F. J., Errandonea, D., Pellicer-Porres, J., Muñoz, V., Tobias, G., Ordejón, P., Canadell, E., San Miguel, A. & Sánchez-Portal, D. (2003). *Phys. Status Solidi B*, **235** 267–276.
Takemura, K. (1995). *Phys. Rev. Lett.* **75**, 1807–1810.
Takemura, K. (1997). *Phys. Rev. B*, **56**, 5170–5179.
Takemura, K. (1999). *Phys. Rev. B*, **60**, 6171–6174.
Takemura, K., Hiroshi, Y., Hiroshi, F. & Takumi, K. (2002). *Phys. Rev. B*, **65**, 132107.
Vidal, O., De Andrade, V., Lewin, E., Muñoz, M., Parra, T. & Pascarelli, S. (2006). *J. Metamorph. Geol.* **24**, 669–683.
Wood, B. J., Walter, M. J. & Wade, J. (2006). *Nature (London)*, **441**, 825–833.